NIH Public Access
Author Manuscript
J Comp Neurol. Author manuscript; available in PMC 2014 September 04.

Published in final edited form as:
J Comp Neurol. 2014 February 15; 522(3): 609–625. doi:10.1002/cne.23435.

Distribution and Functional Expression of Kv4 Family α Subunits and Associated KChIP β Subunits in the Bed Nucleus of the Stria Terminalis

Donald G. Rainnie[1,2,*], **Rimi Hazra**[1,2], **Joanna Dabrowska**[1,2], **Ji-Dong Guo**[1,2], **Chen Chen Li**[1,2], **Sarah Dewitt**[1,2], and **E. Chris Muly**[1,3,4]

[1]Department of Psychiatry and Behavioral Sciences, Emory University, Atlanta, Georgia

[2]Division of Behavioral Neuroscience and Psychiatric Disorders, Yerkes National Primate Research Center, Atlanta, Georgia

[3]Division of Neuropharmacology and Neurological Diseases, Yerkes National Primate Research Center, Atlanta, Georgia

[4]Atlanta Department of Veterans Affairs Medical Center, Decatur, Georgia

Abstract

Regulation of $BNST_{ALG}$ neuronal firing activity is tightly regulated by the opposing actions of the fast outward potassium current, I_A, mediated by α subunits of the Kv4 family of ion channels, and the transient inward calcium current, I_T. Together, these channels play a critical role in regulating the latency to action potential onset, duration, and frequency, as well as dendritic back-propagation and synaptic plasticity. Previously we have shown that Type I–III $BNST_{ALG}$ neurons express mRNA transcripts for each of the Kv4 α subunits. However, the biophysical properties of native I_A channels are critically dependent on the formation of macromolecular complexes of Kv4 channels with a family of chaperone proteins, the potassium channel-interacting proteins (KChIP1–4). Here we used a multidisciplinary approach to investigate the expression and function of Kv4 channels and KChIPs in neurons of the rat $BNST_{ALG}$. Using immunofluorescence we demonstrated the pattern of localization of Kv4.2, Kv4.3, and KChIP1–4 proteins in the $BNST_{ALG}$. Moreover, our single-cell reverse-transcription polymerase chain reaction (scRT-PCR) studies revealed that mRNA transcripts for Kv4.2, Kv4.3, and all four KChIPs were differentially expressed in Type I–III $BNST_{ALG}$ neurons. Furthermore, immunoelectron microscopy revealed that Kv4.2 and Kv4.3 channels were primarily localized to the dendrites and spines of $BNST_{ALG}$ neurons, and are thus ideally situated to modulate synaptic transmission. Consistent with this

© 2013 Wiley Periodicals, Inc.

*CORRESPONDENCE TO: Donald G. Rainnie, Ph.D., Department of Psychiatry and Behavioral Sciences, Yerkes National Primate Research Center, Emory University, Atlanta, GA 30322. drainni@emory.edu.

CONFLICT OF INTEREST

None of the authors have any known or potential conflict of interest including any financial, personal, or other relationships with other people or organizations that could inappropriately influence, or be perceived to influence, this study.

ROLE OF AUTHORS

All authors had full access to all the data in the study and take responsibility for the integrity of the data and the accuracy of the data analysis. Study concept and design: DGR and ECM. Acquisition of data: JD, RH, CCL, JDG, SD, ECM. Analysis and interpretation of data: DGR, ECM, JD, JDG. Drafting of the article: DGR. Critical revision of the article for important intellectual content: DGR, ECM. Statistical analysis: DGR, JDG. Obtained funding: DGR, ECM. Study supervision: DGR.

NIH-PA Author Manuscript
NIH-PA Author Manuscript
NIH-PA Author Manuscript

NIH-PA Author Manuscript

NIH-PA Author Manuscript

NIH-PA Author Manuscript

observation, in vitro patch clamp recordings showed that reducing postsynaptic I_A in these neurons lowered the threshold for long-term potentiation (LTP) induction. These results are discussed in relation to potential modulation of I_A channels by chronic stress.

INDEXING TERMS

patch clamp; LTP; single cell RT-PCR; electron microscopy; voltage-dependent potassium channel

---

Activation of neurons in the anterolateral cell group of the bed nucleus of the stria terminalis ($BNST_{ALG}$) is thought to play a pivotal role in the anxiogenic response to psychological and physical stressors (for review, see Hammack et al., 2009; Walker et al., 2009b). Recently, we have shown that the firing properties and subthreshold intrinsic membrane excitability of the majority of $BNST_{ALG}$ neurons are critically dependent on an interplay between the voltage-dependent transient inward calcium current, I_T, and the voltage-dependent transient outward potassium current, I_A (Hammack et al., 2007). While I_T is depolarizing and promotes action potential generation, I_A acts in opposition to I_T and can delay the onset to action potential firing and limit the number of spikes elicited in response to excitatory input.

The family of voltage-gated potassium channels, referred to as Kv, is a heterogeneous group (Song, 2002), with each channel consisting of four pore-forming α subunits, and multiple accessory subunits. To date, four subfamilies of genes encoding Kv α subunits have been identified: Kv1, Kv2, Kv3, and Kv4, and each subfamily contains multiple members (Yu et al., 2005). In heterologous expression systems, specific Kv α subunits have been shown to form functional channels that have properties similar to physiologically defined A-type potassium channels, namely, the Kv1.4, Kv3.4, and Kv4.1–4.3 subunits (Serodio et al., 1996; Coetzee et al., 1999). Moreover, recent immunohistochemical and biophysical evidence suggests that most of the somatodendritic I_A in central neurons is carried by the Kv4 subfamily of α subunits (for review, see Sheng et al., 1992; Birnbaum et al., 2004; Jerng et al., 2004).

Significantly, the biophysical properties of A-type potassium channels composed of only the pore-forming α subunits when expressed in heterologous systems do not match the properties of the I_A observed in native neuronal systems (Serodio and Rudy, 1998; Holmqvist et al., 2001; Decher et al., 2001; Malin and Nerbonne, 2001). This discrepancy is due to the requirement for auxiliary β subunits not present in these experiments. It is now known that several auxiliary subunits associate with the α subunits to form a macromolecular complex (see Shibata et al., 2003; Birnbaum et al., 2004; Zagha et al., 2005; Jerng et al., 2005), and that association with these auxiliary subunits regulates not only the biophysical properties of the I_A channels, but also their cellular distribution and density within the plasma membrane. Included among the auxiliary subunits are the Kvβ subunits (Kvβ1–Kvβ3), a family of membrane bound dipetidyl peptidase proteins (DPPX and DPP10), as well as a family of potassium channel interacting proteins (KChIPs). Importantly, the KChIPs contain an ef-hand domain and act as calcium binding proteins (Burgoyne and Weiss, 2001). Binding of calcium to KChIPs is reported to facilitate the transport of Kv4 α subunits from the endoplasmic reticulum to the plasma membrane

NIH-PA Author Manuscript

NIH-PA Author Manuscript

NIH-PA Author Manuscript

(Shibata et al., 2003; Chen et al., 2006a). Given the key role played by opposing I_A and I_T channels in regulating firing activity of $BNST_{ALG}$ neurons (Hammack et al., 2007), it is possible that the KChIPs may help to regulate the firing pattern of these neurons by determining the level of somatodendritic I_A channel expression. To date, four KChIPs have been identified (KChIP1–KChIP4), each of which shows differential distribution within the central nervous system (CNS (Xiong et al., 2004; Rhodes et al., 2004; Dabrowska and Rainnie, 2010). Coexpression of the KChIPs with members of the Kv4 family has been shown to promote cell surface expression and increase peak current density, as well as increase the rate of recovery from inactivation (An et al., 2000; Birnbaum et al., 2004).

Recently, we reported that three electrophysiologically distinct cell types (Type I–III) exist in the dorsal portion of the $BNST_{ALG}$ including the oval, juxtacapsular, and rhomboid nuclei and anterolateral area (Hammack et al., 2007). It should be noted, however, that most recording were centered on the oval nucleus. Type I neurons are characterized by a regular firing pattern in response to membrane depolarization, and a depolarizing sag in the voltage response to hyperpolarizing current injection that is mediated by the hyperpolarization-activated cation current, I_h. Type II neurons are characterized by a burst-firing pattern that is mediated by activation of the low-threshold calcium current, I_T, and also express a prominent I_h. Type III neurons are characterized by a regular firing pattern, have no prominent I_h, and a pronounced fast hyperpolarization-activated voltage rectification indicative of the inwardly rectifying potassium current, $I_{K(IR)}$. Because the firing activity of $BNST_{ALG}$ neurons is critically dependent on the interplay between I_A and I_T, we hypothesized that Type I–III neurons may differentially express at least one member of the Kv4 subfamily of α subunits, which could in turn form a macromolecular complex with one or more of the KChIPs. In this way the KChIP auxiliary protein could act as a feedback regulator of I_A expression by sensing enhanced calcium influx through I_T during periods of heightened excitability. More recently, we have shown that mRNA transcripts for the different Kv4 α subunits are differentially expressed by neurons in the $BNST_{ALG}$ (Hazra et al., 2011b). Here, we extend this observation and using molecular biological, immunofluorescence, electron microscopic, and electrophysiological techniques demonstrate that Type I–III $BNST_{ALG}$ neurons differentially coexpress distinct Kv4 and KChIP subunits and that the Kv4 subunits are located in the somatodendritic compartment of these neurons. Furthermore, we show that expression of I_A in $BNST_{ALG}$ neurons regulates action potential threshold and half-width, and that attenuating Kv4 channel function lowered the threshold for induction of synaptic plasticity in these neurons.

MATERIALS AND METHODS

Animals

Male Sprague-Dawley rats (5–7 weeks old, Charles River, Raleigh, NC) were used in these experiments. Animals were housed 4–5 per cage with ad libitum access to food and water. All procedures in used in this study were performed according to the National Institutes for Health *Guide for the Care and Use of Laboratory Animals* and were approved by the Institutional Animal Care and Use Committee of Emory University.

NIH-PA Author Manuscript

NIH-PA Author Manuscript

NIH-PA Author Manuscript

Identification and localization of Kv4 and KChIP subunits in the $BNST_{ALG}$

Whole-tissue mRNA expression—To examine the expression of Kv4 and KChIP subunit mRNA transcripts in isolated BNST tissue, 350-μm coronal sections containing the BNST were prepared from six rats as previously described (Hammack et al., 2007; Guo et al., 2009), and the BNST excised by microdissection. Total RNA was isolated by homogenizing each BNST sample in Trizol (Invitrogen, Carlsbad, CA). The isolated RNA was then reverse-transcribed using a cocktail containing 5–8 μl of 2XRT buffer, 10 mM dNTP mix, 2X random hexanucleotide, Multiscribe RT 5 U/μl, and RNase free water. The mixture was incubated in a PTC-200 Peltier thermal cycler (MJ Research, Water-town, MA) at 25°C for 10 minutes and then 37°C for 120 minutes. The resultant cDNA samples were stored at −20°C until needed. All reagents used in these experiments were obtained from Applied Biosystems (Foster City, CA).

Qualitative polymerase chain reaction (PCR)—Standard PCR was performed on samples of the cDNA using protocols that have been described previously (Hazra et al., 2011b; Guo et al., 2012). The sequences for the oligonucleotide primers used in this study are given in Table 1. In order to reduce intersample variation, each experiment was repeated six times with different rat samples and each sample was assayed in triplicate.

Whole tissue protein expression: immunofluorescence

Tissue processing—Immunofluorescence experiments were performed on 4% paraformaldehyde-fixed rat brain sections derived from six adult (60 days old) rats according to protocols described previously (Dabrowska and Rainnie, 2010; Dabrowska et al., 2011). Briefly, to determine Kv4 and KChIP immunoreactivity in serial brain sections containing the BNST (Bregma +0.13 mm to Bregma −0.53 mm), free-floating sections were permeabilized with 0.5% Triton-X in phosphate-buffered saline (PBS) for 1 hour and then incubated for 48 hours at 4°C with primary antibody in 0.5% Triton-X/PBS solution. Sections were then rinsed 3× for 10 minutes in PBS and incubated at room temperature for 2 hours with either Alexa-Fluor 488 goat antimouse IgG or Alexa-Fluor 568 goat antirabbit IgG (1:500, Molecular Probes, Invitrogen, Carlsbad, CA) depending on the host for the primary antibody. Sections were then rinsed 3× for 10 minutes in PBS, and 1× in phosphate buffer (PB), mounted on gelatin-coated glass slides, and coverslipped using Vectashield mounting medium (Vector Laboratories, Burlingame, CA). High-resolution photomicrographs were obtained using spinning disc confocal laser microscopy and an Orca R2 cooled CCD camera (Hammamatsu, Bridgewater, NJ) mounted on a Leica DM5500B microscope (Leica Microsystems, Bannockburn, IL).

All of the primary antibodies used in this study have been described in detail elsewhere (Dabrowska and Rainnie, 2010). Antibodies against the α (Kv4.2, Kv4.3) and β subunits (KChIP1, KChIP2, and KChIP3) were produced by the UC Davis/NIH NeuroMab Facility and sold under license by Antibodies Inc. (Davis, CA). The KChIP4 antibody was purchased from Abcam (Cambridge, MA). Table 2 outlines the specific details of the antibodies used in this study.

NIH-PA Author Manuscript

NIH-PA Author Manuscript

NIH-PA Author Manuscript

Verification of antibody specificity and quantification of protein levels—The antibodies used in these experiments are listed in Table 2, along with their source and the specific antigen used in their preparation. The NeuroMab Kv4.2 antibody stained a single band with a molecular weight of 70 kD on western blots and no labeling on western blot or immunofluorescence staining of rat hippocampal sections was seen in knockout mouse tissue (manufacturer's technical information). The NeuroMab Kv4.3 antibody stained a single band with a molecular weight of 75 kD on western blots and no labeling on western blot was seen in knockout mouse tissue (manufacturer's technical information). The NeuroMab KChIP1 antibody stained a double band with a molecular weight of ~30 kD on western blots and no crossreactivity with KChIP2, 3, or 4 was observed (manufacturer's technical information). The NeuroMab KChIP2 antibody stained a single band with a molecular weight of ~35 kD on western blots and no crossreactivity with KChIP1 or 3 was observed (manufacturer's technical information). The NeuroMab KChIP3 antibody stained a single band with a molecular weight of 37 kD on western blots and no labeling on western blot was seen in knockout mouse tissue (manufacturer's technical information). The Abcam KChIP4 antibody stained a single band with a molecular weight of ~54 kD on western (manufacturer's technical information).

Electron microscopy—For the immunoelectron microscopy studies, eight rats were sacrificed and perfused with 4% paraformaldehyde, 0.2% glutaraldehyde, and 0.2% picric acid in PBS. The brains were blocked and postfixed in 4% paraformaldehyde for 4 hours. Coronal, 50-μm thick vibratome sections were cut and stored frozen at −80°C in 15% sucrose until immunohistochemical experiments were performed. Single-label immunoperoxidase labeling was performed as described previously (Muly et al., 2003). Briefly, sections were thawed, incubated in blocking serum (3% normal goat serum, 1% bovine serum albumin, 0.1% glycine, 0.1% lysine in 0.01 M PBS, pH 7.4) for 1 hour, and then placed in primary antiserum diluted in blocking serum. After 36 hours at 4°C, the sections were rinsed and placed in a 1:200 dilution of biotinylated goat antirabbit IgG (Jackson ImmunoResearch, West Grove, PA) or biotinylated horse antimouse IgG (Vector, Burlingame, CA) for 1 hour at room temperature. The sections were then rinsed, placed in ABC Elite (Vector) for 1 hour at room temperature, and then processed to reveal peroxidase using 3,3′-diamino-benzidine (DAB) as the chromagen. Sections were then postfixed in osmium tetroxide, stained *en bloc* with uranyl acetate, dehydrated, and embedded in Durcupan resin (Electron Microscopy Sciences, Fort Washington, PA). Selected regions of the BNST were mounted on blocks and ultrathin sections were collected onto pioloform-coated slot grids and counterstained with lead citrate. Control sections processed as above except for the omission of the primary immunoreagent did not contain DAB label upon electron microscopic examination.

Ultrathin sections were examined with a Zeiss EM10C electron microscope and immunoreactive elements were imaged using a Dualvision cooled CCD camera (1300 × 1030 pixels) and Digital Micrograph software (v. 3.7.4, Gatan, Pleasanton, CA). Labeled profiles were identified using established morphological criteria (Muly et al., 2003). Images selected for publication were saved in TIFF format and imported into an image processing

NIH-PA Author Manuscript

NIH-PA Author Manuscript

NIH-PA Author Manuscript

program (Canvas 8; Deneba Software, Miami, FL). The contrast was adjusted and the images were cropped to meet size requirements.

Cellular expression and physiology

Tissue preparation and patch clamp recording—Slices containing the $BNST_{ALG}$ were obtained as previously described (Rainnie, 1999; Muly et al., 2007; Guo et al., 2009). Briefly, under deep isoflurane anesthesia, animals were decapitated and the brain rapidly removed and immersed in cold (4°C) 95%–5% oxygen/carbon dioxide oxygenated "cutting solution" with the following composition (in mM): NaCl (130), $NaHCO_3$ (30), KCl (3.50), KH_2PO4 (1.10), $MgCl_2$ (6.0), $CaCl_2$ (1.0), glucose (10), supplemented with kynurenic acid (2.0). Slices containing the BNST were cut at a thickness of 350 μm using a Leica VTS-1000 vibratome (Leica Microsystems). Slices were kept in oxygenated "cutting solution" at room temperature for 1 hour before transferring to regular artificial cerebrospinal fluid (ACSF) containing (in mM): NaCl (130), $NaHCO_3$ (30), KCl (3.50), KH_2PO_4 (1.10), $MgCl_2$ (1.30), $CaCl_2$ (2.50), and glucose (10). Slices were then placed in regular ACSF for at least 30 minutes before recording.

To record I_A from BNST neurons and conduct single-cell reverse-transcription polymerase chain reaction (scRT-PCR) studies, individual slices were transferred to a recording chamber mounted on the fixed stage of a Leica DMLFS microscope (Leica Microsystems). The slices were maintained fully submerged and continuously perfused at 1–2 ml/s with oxygenated ACSF at 32°C. Individual cells were identified by using differential interference contrast (DIC) optics and infrared (IR) illumination with an IR-sensitive CCD camera (Orca ER, Hamamatsu, Tokyo Japan). Patch pipettes were pulled from borosilicate glass and had a resistance of 4–6 MΩ. The recording patch solution had the following composition (in mM): 130 K-gluconate, 2 KCl, 10 HEPES, 3 $MgCl_2$, 2 K-ATP, 0.2 NaGTP, and 5 phosphocreatine, titered to pH 7.3 with KOH, and 290 mOsm. Data acquisition and analysis were performed using a MultiClamp 700B amplifier (Molecular Devices, Union City, CA) in conjunction with pClamp 10.0 software and a DigiData 1320A AD/DA interface (Molecular Devices). Whole-cell patch clamp recordings were obtained using standard methods and whole cell currents were then filtered at 2 kHz and digitized at 5 kHz. For most experiments the membrane potential was held at −60 mV unless otherwise stated. The access resistance was monitored throughout each experiment and neurons that had a >15% change in access resistance were discarded.

I_A recording and analysis—Isolation of the I_A in $BNST_{ALG}$ neurons was performed as previously described by Riazanski et al. (2001). Briefly, after the establishment of whole-cell recording mode, the standard ACSF was substituted with an "I_A ACSF" of the following composition (in mM): NaCl (110), $NaHCO_3$ (24), TEA-Cl (20), KCl (3.50), KH_2PO_4 (1.10), $MgCl_2$ (3.30), $CaCl_2$ (0.50), $CdCl_2$ (0.15), $NiCl_2$ (0.5) TTX (1), and glucose (10). To determine the voltage dependency of activation and inactivation of I_A, dual step protocols were applied and a subtraction method was used to isolate I_A. To determine I_A activation, the membrane potential was stepped to −110 mV for 400 ms, and then stepped from −70 mV to +70 mV in increments of 20 mV for 300 ms. To allow subsequent I_A isolation, the protocol was then repeated with a 200-ms step to −20 mV to fully inactivate I_A

NIH-PA Author Manuscript

NIH-PA Author Manuscript

NIH-PA Author Manuscript

inserted prior to initiating the depolarizing step command. To isolate I_A, currents generated with I_A inactivated were then digitally subtracted from those with I_A present. Steady-state I_A inactivation was determined using a second dual-step protocol. Briefly, the membrane potential was stepped to −100 mV followed by a series of transient (200 ms) step commands from −120 mV to +60 mV, which were followed immediately by step command to +30 mV. The peak amplitude of I_A was calculated as the difference between peak current and the current at the end of command pulse. The voltage dependency of steady-state inactivation and activation of I_A were then determined by plotting normalized peak amplitude, or conductance, respectively, as a function of the command step potential.

Conductance was calculated as:

$$\mathrm{G(V)=I(V)/(V-V_K)}$$

where *V* is holding potential and V_K is potassium reversal potential.

G(V) was then fit with a Boltzmann equation:

$$G(V)=\frac{G\max}{1+\exp\left[\left(V-V^{\frac{1}{2}}\right)/k\right]},$$

where *Gmax* is the maximum K^+ conductance, $V_{1/2}$ is half-maximal membrane potential, and *k* is the slope factor.

To determine the time constant of I_A decay (tau) the decay phase of the isolated I_A elicited with command steps to +30 mV was fit by a single exponential curve. Tau was determined as the time taken to reach 1/e of the peak current.

To determine the role of Kv4 channels in mediating the isolated I_A, increasing concentrations of 4-AP (50 μM to 10 mM) were applied to BNST neurons and the dose–response relationship was calculated by fitting the resulting data with a Hill equation and then determining IC_{50}.

To determine the functional implications of I_A expression in $BNST_{ALG}$ neurons, we examined the effects of intracellular application of 4-AP on the passive and active membrane properties of Type I–III neurons. Here, 4-AP (500 μM) was included in the patch solution and standard protocols were used to determine the membrane properties.

Long-term potentiation (LTP) induction—The ability of high-frequency stimulation (HFS) to induce LTP in $BNST_{ALG}$ in the presence or absence of I_A channel blockers was evaluated using a subthreshold stimulation paradigm reported in detail elsewhere (Li et al., 2011). Briefly, monosynaptic excitatory postsynaptic currents (EPSCs) were evoked by electrical stimulation of stria terminalis using a concentric stimulation electrode (CBBPF100; Frederick Haer, Bowdoinham, ME). In all experiments the $GABA_A$ antagonist SR 95531 (5 μM) was included in the ACSF to prevent contamination of stimulus-evoked EPSCs by IPSCs. Stimulation intensity was adjusted to achieve 30% maximal EPSC

NIH-PA Author Manuscript

NIH-PA Author Manuscript

NIH-PA Author Manuscript

amplitude, and baseline EPSCs were recorded at a frequency of 0.05 Hz for 10 minutes. Standard LTP was then induced with five trains of high-frequency stimulation (5× HFS; 100 Hz, 150 μs, 1 sec) applied through the stimulation electrode at 20-second intervals. To examine the effect of reducing I_A on LTP induction, 500 μM 4-AP was included in the patch recording solution and a subthreshold stimulation paradigm was employed in which only two trains of stimuli (2× HFS) were applied. To determine the magnitude of any synaptic plasticity evoked by the two stimulation protocols, the peak amplitude of the EPSC was normalized to the mean value of the baseline EPSC amplitude. A two-way analysis of variance (ANOVA) was used to determine the effect on LTP-induction of including 4-AP in the patch solution.

scRT-PCR—To examine the relative Kv4 and KChIP mRNA expression profile of Type I–III $BNST_{ALG}$ neurons, after recording their physiological properties the cytoplasm of each neuron was aspirated into the patch recording pipette and expelled into a microcentrifuge tube containing reverse transcription (RT) cocktail (Applied Biosystems). The RT product was amplified in triplicate using standard procedures and screened for 18S rRNA. Only cells positive for 18S rRNA were then subjected to amplification with specific primers. The full procedure used to determine the mRNA transcript expression profile in single cells has been described in detail elsewhere (Martin et al., 2010; Hazra et al., 2011b).

RESULTS

Regional distribution of Kv4s and KChIPs in the $BNST_{ALG}$

In order to determine the relative protein distribution of members of the Kv4 family and their associated beta subunit proteins in the $BNST_{ALG}$, we first conducted an immunofluorescence study to determine the distribution pattern for the Kv4 channel α subunits, as well as the four KChIP1–4 subunits. Unfortunately the Kv4.1 α subunit antibody showed two bands in western blots and an apparent nonspecific nuclear staining pattern in and around the BNST and, hence, was omitted from any further analysis in this study. In contrast, as illustrated in Figure 1A,B, at low magnification (10×) both Kv4.2 and Kv4.3 channel α subunit immunoreactivity was observed in the $BNST_{ALG}$, with each subunit showing a slightly different distribution pattern. Although both Kv4.2 and Kv4.3 were found at high levels in the $BNST_{ALG}$, Kv4.2 was more evenly distributed throughout the $BNST_{ALG}$, while the highest immunoreactivity for Kv4.3 was observed in more medial aspects of the $BNST_{ALG}$ (Fig. 1C). At higher magnification (Fig. 1B), Kv4.2 immunoreactivity was seen to be restricted to puncta in the neuropil of the $BNST_{ALG}$ and, to a lesser extent, dendritic processes (arrows, Fig. 1C). In addition to strong neuropil immunoreactivity in the form of puncta, Kv4.3 immunoreactivity also showed clear labeling of cell bodies and processes that appear to be dendrites (arrows, Fig. 1D).

The KChIP β subunit chaperone proteins also showed a differential distribution throughout the $BNST_{ALG}$ (Fig. 2). KChIP1 labeling appeared light in the $BNST_{ALG}$ (Fig. 2A), and was the only β-subunit to show distinct somatodendritic expression in presumed $BNST_{ALG}$ neurons (arrows, Fig. 2B). KChIP2 immunoreactivity was the strongest of all four KChIPs in the $BNST_{ALG}$ (Fig. 2C) and was observed mainly in puncta in the neuropil, as well as in

NIH-PA Author Manuscript

NIH-PA Author Manuscript

NIH-PA Author Manuscript

the soma of presumed neurons (arrows, Fig. 2D). KChIP3 immunoreactivity was also observed in the $BNST_{ALG}$, and it appeared as puncta uniformly distributed throughout the neuropil as well as rings of immunoreactivity that appear to be somatic labeling similar to that seen for KChIP2 (arrows, Fig. 2F). KChIP4 labeling was the lightest of the four (Fig. 2G) and was restricted to puncta in the neuropil of the $BNST_{ALG}$ (Fig. 2H). These data suggest that I_A channels in $BNST_{ALG}$ neurons are molecularly complex, and are comprised of multiple Kv4 α and β subunits.

Single-cell expression of mRNA Transcripts for K_V4 Channel a and b subunits in the $BNST_{ALG}$

The expression of α and β subunits in Type I–III neurons was determined using a combination of whole-cell patch-clamp recording and scRT-PCR in 61 neurons (Table 3). Transcripts for the Kv1.4 and Kv3.4 I_A channel subunits were expressed at low levels, and were only detected in 3/40 Type II and 3/12 Type III $BNST_{ALG}$ neurons (data not shown), suggesting that α subunits of the Kv4 family are the major determinants of I_A channel function in $BNST_{ALG}$ neurons. Moreover, despite having detected a Kv4.1 mRNA signal in $BNST_{ALG}$ whole-tissue homogenates, we failed to detect Kv4.1 transcripts in any of the 61 neurons sampled, suggesting that the signal in the tissue homogenate may be of nonneuronal origin. However, in agreement with our immunofluorescence study, mRNA transcripts for the Kv4.2 subunit were found in the majority of neurons (47/61), and transcripts for Kv4.3 were found in 23/61 neurons (see Table 2).

Interestingly, when the Kv4 and the KChIP data were combined a clear pattern of cell type-specific expression emerged. Thus, Type I neurons express mRNA transcripts for Kv4.2 and Kv4.3, as well as for KChIP3 and KChIP4, but not KChIP1 or KChIP2. Type III neurons could be distinguished from Type I and II neurons in that they were the only group to express mRNA transcripts for Kv4.2 and KChIP2, as well as expressing KChIP4. The situation for Type II neurons is more complex. The majority of Type II neurons (26/43) only expressed transcripts for Kv4.2 and either KChIP3 or KChIP4. The remaining Type II neurons (14/40) were unique in that they were the only subpopulation of $BNST_{ALG}$ neurons to express mRNA transcripts for Kv4.3 in the absence of Kv4.2 and also the only subpopulation to express KChIP1, in addition to all of the other KChIPs. We recently reported that Type II neurons could be differentiated into three subtypes, Type IIA–IIC, based on their serotonin (5-HT) receptor mRNA expression pattern (Hazra et al., 2012). Significantly, these three Type II subtypes showed similar selective expression of Kv4 and KChIP transcripts. Type IIA neurons, which predominantly express transcripts for 5-HT_3 and 5-HT_7 receptors, express only Kv4.2 and KChIP3. Type IIB, which mainly express 5-HT_{1B} and 5-HT_4 receptors, express Kv4.2 and KChIP4. While Type IIC neurons, which predominantly express transcripts for 5-HT_{1A} and 5-HT_{2A} receptors, express Kv4.3 and all four types of KChIP. Consequently, we will adopt this terminology here (see Table 3). Together, these data demonstrate that the expression of Kv4 α and β subunits in $BNST_{ALG}$ neurons is not uniform, but that it correlates with identifiable physiological phenotypes and 5-HT receptor expression patterns.

NIH-PA Author Manuscript

NIH-PA Author Manuscript

NIH-PA Author Manuscript

Subcellular localization of Kv4 α subunit proteins in the $BNST_{ALG}$

Having established that Kv4.2 and Kv4.3 are the major components of neuronal I_A channels in the $BNST_{ALG}$, we next used immunoelectron microscopy to examine the subcellular localization of these subunits. The Kv4.3-labeled profiles were found primarily in dendrites (Fig. 3C), consistent with the prominent labeling of processes in our immunofluorescence experiment. As predicted by our immunofluorescence and scRT-PCR studies, the distribution of label for Kv4.2 was more complex than Kv4.3. Again, labeled dendrites appeared to be the most frequently observed, but spines were also commonly labeled (Fig. 3A). Finally, glial processes were also immunoreactive for Kv4.2 (Fig. 3B). These observations confirm that the Kv4 channels are located on the dendritic arbor of $BNST_{ALG}$ neurons, with some degree of localization in dendritic spines; moreover, the relative frequency of labeling in dendritic spines appears to be higher for Kv4.2 than Kv4.3.

Physiologic consequences of Kv4-medited I_A modulation in $BNST_{ALG}$ neurons

We next undertook a series of electrophysiological studies to better define the functional characteristics of I_A in $BNST_{ALG}$ neurons. First we examined the voltage dependency of activation and inactivation of I_A in $BNST_{ALG}$ neurons. As illustrated in Figure 4A, I_A was isolated using a digital subtraction protocol, similar to that previously described by Riazanski et al. (2001). Here, traces in which I_A had been inactivated by a transient (200 ms) step to −20 mV (middle two traces) were subtracted from those with no prior inactivation step (upper two traces). A typical series of the resulting isolated I_A is illustrated in Figure 4A (bottom trace), and when fit by a single exponential curve revealed a tau of 25.8 ± 0.9 ms with command steps to +30 mV (n =30). For both the activation (Fig. 4A) and inactivation (Fig. 4B) protocols, peak I_A was calculated by subtracting the current at the end test pulse from the peak at its onset. Figure 4C shows the normalized group data for inactivation and activation curves fit with Boltzmann equations. Half-maximal activation and inactivation were found to be 12.2 ± 1.1 mV and −24.8 ± 1.2mV, respectively (n =30, see Table 4).

We then examined the dose–response relationship for 4-AP blockade of the isolated I_A in these neurons. As seen in Figure 4D, 4-AP caused a dose-dependent reduction in the peak amplitude of I_A, with full block only occurring at millimolar concentrations. A plot of normalized peak I_A as a function of 4-AP concentration revealed an IC_{50} = 460 μM (Fig. 4E), a figure intermediate between low sensitivity Kv4 family subunits and high sensitivity Kv1 and Kv3 subunits. This raises the possibility that although Kv4.2 and 4.3 α channel subunits may predominate in these neurons; Kv1.4/3.4 α subunits may also contribute to I_A.

Because our scRT-PCR results revealed that mRNA for the Kv4 channel subunits were differently expressed in Type I–III $BNST_{ALG}$ neurons, we next compared the functional properties of I_A in each of the three subtypes. The group data for the voltage-dependent activation and inactivation curves for Type I–III neurons is shown in Figure 5. While a two-way ANOVA indicated a significant effect of voltage ($F_{7,216}$ = 574, $P < 0.001$) on activation, no significant difference was observed with cell type ($F_{2,216}$ = 1.2, $P > 0.05$), and there was no significant interaction between voltage and cell type ($F_{14,216}$ = 0.97, $P > 0.05$). For the inactivation plot, two-way ANOVA revealed a significant effect of voltage ($F_{9,260}$ =

NIH-PA Author Manuscript

NIH-PA Author Manuscript

NIH-PA Author Manuscript

318, $P < 0.001$) and cell type ($F_{2,260} = 3.68$, $P < 0.05$), but no significant interaction of voltage and cell type ($F_{18,260} = 0.66$, $P > 0.05$). The properties of the isolated I_A in Type I–III BNST neurons are summarized in Table 4. Although there was a trend towards Type II neurons having a higher peak I_A amplitude than Type I and III neurons, it did not reach statistical significance. Given that Type II neurons are a heterogeneous cell population, it is possible that a select subgroup may be driving this trend.

We next examined the effects of reducing I_A amplitude on the threshold for LTP induction in BNST neurons by including 4-AP in the patch recording (McDermott and Schrader, 2011). First, we determined the effect of inclusion of 500 μM 4-AP in the patch solution on the passive and active membrane properties of $BNST_{ALG}$ neurons. As illustrated in Figure 6A,B, 4-AP caused a significant reduction in the amplitude of the isolated I_A, together with a hyperpolarizing shift in the threshold for action potential generation and a broadening of the action potential half-width (Fig. 6C). Because of the differential expression of Kv4 subunits in Type I–III neurons, we were interested to see if there was any differential sensitivity to the 4-AP manipulation across cell types. However, because 4-AP had a direct effect on the firing pattern of $BNST_{ALG}$ neurons it was difficult to differentiate between cell types using this as a criterion. Consequently, we were restricted to using the voltage response to transient hyperpolarizing current injection as the criterion for distinguishing Type I/II from Type III neurons. Type III neurons were clearly distinguishable from Type I/II neurons by the absence of a time-dependent depolarizing sag in the voltage traces elicited in response to transient hyperpolarizing current injection (Hammack et al., 2007). Table 5 summarizes the grouped data comparing the effect of intracellular 4-AP on the properties of Type I/II and Type III neurons. Blockade of I_A significantly increased the action potential half-width and lowered spike threshold in both cell groups.

Next, we induced LTP in $BNST_{ALG}$ neurons using a classic 5× HFS protocol (see Materials and Methods). The grouped response to 5× HFS is illustrated in Figure 6D (filled diamonds). In agreement with previous studies (Weitlauf et al., 2004; Kash et al., 2008; Conrad et al., 2011) 5× HFS of the stria terminalis caused a long-lasting potentiation of the amplitude of evoked EPSCs (~50% above baseline, $n = 8$) in all $BNST_{ALG}$ neurons tested, irrespective of cell type, which lasted for at least 40 minutes. In contrast, subthreshold stimulation (2× HFS) failed to induce LTP in any $BNST_{ALG}$ neuron tested (Fig. 6D, open triangles; $n = 5$). Significantly, when 500 μM 4-AP was included in the patch recording solution 2× HFS routinely induced LTP in all neurons tested (~35% above baseline, Fig. 6D, inverted triangles; $n = 10$), irrespective of cell type. Two-way repeated measures ANOVA indicated a significant drug effect ($F_{(1,533)} = 6.9$, $P < 0.01$), and a significant effect of time ($F_{(40,533)} = 3.5$, $P < 0.01$), but no significant interaction between 4-AP and time ($F_{(40,533)} = 0.28$, $P > 0.05$). Consistent with results from the hippocampus, these results suggest that the Kv4 family of I_A channels may play a significant role in regulating the threshold for LTP induction in $BNST_{ALG}$ neurons.

DISCUSSION

In the current study we used a multidisciplinary approach combining immunohistochemical, molecular biological, electron microscopic, and electrophysiological techniques to

NIH-PA Author Manuscript

NIH-PA Author Manuscript

NIH-PA Author Manuscript

demonstrate that Type I–III $BNST_{ALG}$ neurons differentially express distinct combinations of Kv4 and KChIP subunits, and that the Kv4.2 and Kv4.3 α subunits are expressed in the somatodendritic compartment of these neurons. Furthermore, we show that attenuation of Kv4 channel activity in Type I–III neurons significantly increased the action potential half-width and reduced the threshold for action potential generation. Consistent with this observation, attenuating Kv4 channel function also lowered the threshold for induction of synaptic plasticity in these neurons. Given the pivotal role played by $BNST_{ALG}$ neurons in the behavioral response to acute psychological and physical stressors, and the growing recognition that functional disruption of subpopulations of these neurons most likely contributes to the etiology of anxiety disorders and posttraumatic stress disorder (PTSD), the results from the current study suggest that manipulations selectively targeting Kv4.2 and/or Kv4.3 channels subunits and their associated KChIP β subunits may represent novel targets for managing stress-induced affective disorders.

The principal neurochemical phenotype of Type I–III neurons of the $BNST_{ALG}$ is GABAergic (Hazra et al., 2011b; Dabrowska et al., 2011), and though a part of the extended amygdala (De Olmos and Heimer, 1999), the BNST has been argued to be a component of the striatal system (Swanson and Petrovich, 1998). It is not surprising, therefore, that expression of the Kv4 and KChIP peptide subunits mirrors that previously reported in the striatum (Serodio and Rudy, 1998; Xiong et al., 2004; Rhodes et al., 2004). Specifically, we found that while Kv4.2 and KChIP2 appear to be expressed most abundantly in the $BNST_{ALG}$, Kv4.3 and KChIP1 were the only subunits to show a clear somatodendritic staining pattern. The same pattern of staining is seen in the striatum, where it has been suggested that Kv4.3 and KChIP1 may selectively label a subpopulation of large, multipolar, somatostatin (SST) or neuropeptide Y (NPY) containing interneurons (Rhodes et al., 2004). Similarly, distinct subpopulations of peptidergic interneurons in the hippocampus (Menegola and Trimmer, 2006; Bourdeau et al., 2011) and basolateral amygdala (Dabrowska and Rainnie, 2010) also selectively express Kv4.3 and KChIP1. Hence, coexpression of Kv4.3 and KChIP1 may represent a marker for a class of interneurons across brain regions. Consistent with this hypothesis, our scRT-PCR study revealed that the expression of mRNA transcripts for both Kv4.3 and KChIP1 in the $BNST_{ALG}$ was restricted to a unique subpopulation of Type II neurons, namely, Type IIC neurons, and recently we demonstrated that Type IIC neurons also coexpress mRNA transcripts for SST, NPY, and the endogenous opioid neurotransmitter, dynorphin (Hazra et al., 2011a).

In agreement with our immunofluorescence and scRT-PCR studies, results from our electron microscopy study suggest that expression of the Kv4.2 α subunit is higher than that of the Kv4.3 subunit, and more widely distributed in the $BNST_{ALG}$. Significantly, expression of the Kv4.2 subunit was observed in glia, suggesting that modulation of Kv4.2 channel activity would have a more complex effect on cell function in the BNST than that of Kv4.3. Consistent with this observation, both Kv4 α subunits and KChIPs are reportedly expressed by cultured hippocampal astrocytes (Bekar et al., 2005) and Muller glial cells of the retina (Chavira-Suarez et al., 2011). Moreover, whereas the signal for Kv4.3 was observed primarily in dendrites, the Kv4.2 signal was observed in both the dendrites and spines of $BNST_{ALG}$ neurons. Dendritic spines are believed to be the primary point of contact for

NIH-PA Author Manuscript

NIH-PA Author Manuscript

NIH-PA Author Manuscript

excitatory synaptic input onto most CNS neurons (Bhatt et al., 2009), hence expression of Kv4.2 in the spines of these neurons would suggest that Kv4.2 channel activity could directly regulate excitatory synaptic transmission in these neurons. Consistent with this premise, Kv4.2 gene deletion results in a lowering of the threshold for LTP induction in hippocampal CA1 neurons (Chen et al., 2006b), and an enhanced time window in which theta burst stimulation will induce LTP (Zhao et al., 2011). We have shown a similar effect of lowering the threshold for LTP induction in $BNST_{ALG}$ neurons by attenuating I_A channel function with intracellular 4-AP application. Significantly, LTP itself has been shown to cause an activity-dependent internalization of Kv4.2 channels to enhance synaptic transmission, an effect that can be mimicked by reducing Kv4.2 expression with a dominant-negative gene knockdown (Jung et al., 2008). Thus, I_A mediated by Kv4.2 subunits in dendritic spines might be important regulators of synaptic plasticity for individual inputs onto BNST neurons.

Recently, Nerbonne and colleagues demonstrated that Kv4.2 and Kv4.3 also play distinct roles in regulating the firing properties of cortical pyramidal neurons (Carrasquillo et al., 2012) such that in vivo deletion of Kv4.2 resulted in an increase in the membrane input resistance (Rm) as well as reducing the threshold for action potential generation and broadening the action potential half-width. Consistent with this observation, we have shown that reduction of I_A in $BNST_{ALG}$ neurons also significantly increased action potential half-width and reduced action potential threshold. While there was a trend toward an increase in Rm in Type III neurons from 254 ± 60 to 349 ± 111 MΩ following blockade of I_A the change did not reach statistical significance.

As we previously reported for Kv4 subunits, our scRT-PCR data revealed that the four KChIP proteins are differentially expressed in subpopulations of $BNST_{ALG}$ neurons. Thus, membrane expression of I_A channels in Type I neurons would appear to be preferentially regulated by KChIP3 and KChIP4. In Type IIA and IIB neurons, I_A channel activity would be regulated by either KChIP3 or KChIP4, respectively. Intriguingly, Type IIC neurons, which are the only cell population to express the Kv4.3 a subunit and not the Kv4.2 a subunit, express all four of the KChIP subunits. Nerbonne and colleagues have shown that, in cortical neurons expressing KChIP2–4 subunits, deletion of a single KChIP isoform has little effect on I_A density, and in fact other isoforms may compensate for the loss by upregulation (Norris et al., 2010). Marked remodeling of I_A only occurred with a triple gene deletion. Hence, Type IIC neurons may be preferentially buffered against perturbations of KChIP expression compared to most of the other BNST neuronal subtypes. Type III neurons also express multiple KChIP isoforms, predominantly KChIP2 and KChIP4, but with additional low-level expression of KChIP3. Hence, these neurons would also be expected to be relatively well buffered against perturbations of the KChIP system.

Alternatively, expression of multiple KChIP isoforms in a single neuronal population may allow region specific targeting of I_A channels to different cellular compartments (Birnbaum et al., 2004). In addition, recent evidence suggests that the different KChIP isoforms can confer a high level of variability in the properties of the I_A channels (for review, see Burgoyne, 2007). Hence, differential expression of the KChIP subunits in subpopulations of $BNST_{ALG}$ neurons may subtly alter the properties of these distinct neuronal populations.

NIH-PA Author Manuscript

NIH-PA Author Manuscript

NIH-PA Author Manuscript

Intriguingly, KChIP3 knockout mice show enhanced LTP in the dentate gyrus and CA1–CA3 regions of the hippocampus that was associated with enhanced memory and a downregulation of a Kv4 channel-dependent I_A (Lilliehook et al., 2003; Alexander et al., 2009; Fontan-Lozano et al., 2009). Similarly, knockout of Kv4.2 resulted in a significant reduction of KChIP2 expression in the striatum, and KChIP2/3 in the hippocampus (Menegola and Trimmer, 2006), suggesting that the cellular fate of the Kv4 and KChIP subunits are functionally linked.

Finally, as EF-hand domain proteins the KChIP subunits can bind calcium and directly regulate cell function by altering the properties of Kv4 channels. Hence, Anderson et al. (2010a,b) reported that Kv4 channels form a signaling complex that includes Kv4, KChIP3, and members of the Ca(V)3 family of T-type calcium channels. Calcium entry through T channels was shown to cause a rightward shift in the inactivation voltage of Kv4 channels, thereby allowing Kv4 channels to operate in a subthreshold membrane potential range to regulate neuronal firing properties. Previously, we have shown that the firing activity of $BNST_{ALG}$ neurons is critically dependent on an interplay between I_A and I_T, and that Type II and Type III neurons express Ca(V)3.1 and Ca(V)3.3, respectively (Hammack et al., 2007; Hazra et al., 2011b). Importantly, these two neuronal subpopulations also express KChIP3 and, hence, the latency to onset of action potential firing may be more dynamically regulated in Type IIA, IIC, and Type III neurons than in Type I neurons.

By binding to calcium, KChIPs can also change cell function independently of their interaction with Kv4 channels, to regulate gene transcription (see Burgoyne and Weiss, 2001). Initially, KChIP3 was recognized to be identical with the transcriptional regulator DREAM (downstream regulatory element antagonist molecule). It is now recognized that all four KChIPs can act as transcriptional regulators (Link et al., 2004; Burgoyne, 2007), and hence, differential expression of KChIP1–4 in the different subpopulations of $BNST_{ALG}$ neurons may add additional complexity to the response of these neurons to calcium influx following neuronal activation. When it is not bound to calcium KChIP3/DREAM binds to DRE (downstream regulatory element) sites on the promoter region of many genes. Binding of KChIP3/DREAM to DRE represses gene transcription; however, when it binds calcium KChIP3/DREAM dissociates from DRE and repression is lost. KChIP3/DREAM can also form a protein–protein interaction with CREB to prevent CRE-dependent transcription (Ledo et al., 2002). Hence, calcium-dependent regulation of KChIP3/DREAM activity could have a significant influence on activity dependent gene regulation in those $BNST_{ALG}$ neurons that express KChIP3, namely, Type I, Type IIA, Type IIC, and to a lesser extent Type III. Significantly, KChIP3/DREAM has been shown to negatively regulate N-methyl-D-aspartic acid (NMDA) receptor expression (Zhang et al., 2010), and KChIP3/DREAM gene deletion results in enhanced LTP (Lilliehook et al., 2003) and facilitated learning and memory (Fontan-Lozano et al., 2009; Alexander et al., 2009). In contrast, mice expressing a calcium-insensitive KChIP3 mutant show deficits in synaptic depression and contextual fear memory (Wu et al., 2010). It is noteworthy, therefore, that neurons of the $BNST_{ALG}$ show an NMDA receptor-dependent form of LTP (Kash et al., 2008), and that lesions of the BNST induce deficits in contextual fear learning (Sullivan et al., 2004; Zimmerman and Maren, 2011).

NIH-PA Author Manuscript

NIH-PA Author Manuscript

NIH-PA Author Manuscript

Given the broad pattern of expression for the Kv4 α subunits and their associated KChIPs in neurons of the $BNST_{ALG}$, an area known to play a critical role in the behavioral response to environmental stressors, there is reason to believe that factors that modulate I_A may play an important role in pathology and disease. For example, traumatic brain injury has been shown to downregulate I_A in the hippocampus, and is associated with neuronal hyperexcitability, learning deficits, and increased seizure-sensitivity (Lei et al., 2011), suggesting that aberrant I_A function may contribute to neuropathology. Consistent with this observation, neuronal hyperexcitability, learning deficits, and increased seizure-sensitivity are prominent characteristics of Fragile X syndrome (FXS) in which loss of expression of fragile x mental retardation protein (FMRP) results in a significant reduction in Kv4.2 mRNA and protein expression (Gross et al., 2011). Similarly, Kv4.2 knockout mice have learning deficits, and enhanced sensitivity to seizure induction (Barnwell et al., 2009), as well as an enhanced stress response compared to wildtype mice (Lockridge et al., 2010). Hyperactivation of the BNST is reported to mediate sustained anxiety-like behavior in response to environmental stressors (Walker et al., 2009a,b), and hence loss of function of Kv4.2 in $BNST_{ALG}$ neurons may contribute to the behavioral phenotype in the Kv4.2 KO and FXS mice.

Acknowledgments

Grant sponsor: NIMH; Grant number: MH072908 (to D.G.R.); Grant sponsor: Merit Award from the Office of Research and Development, Department of Veterans Affairs (to E.C.M.); Grant sponsor: National Center for Research Resources; Grant number: P51RR169; Grant sponsor: NIH; Grant number: P51 OD011132; Grant sponsor: Office of Research Infrastructure Programs; Grant number: OD P51OD11107.

LITERATURE CITED

Alexander JC, McDermott CM, Tunur T, Rands V, Stelly C, Karhson D, Bowlby MR, An WF, Sweatt JD, Schrader LA. The role of calsenilin/DREAM/KChIP3 in contextual fear conditioning. Learn Mem. 2009; 16:167–177. [PubMed: 19223600]

An WF, Bowlby MR, Betty M, Cao J, Ling HP, Mendoza G, Hinson JW, Mattsson KI, Strassle BW, Trimmer JS, Rhodes KJ. Modulation of A-type potassium channels by a family of calcium sensors. Nature. 2000; 403:553–556. [PubMed: 10676964]

Anderson D, Mehaffey WH, Iftinca M, Rehak R, Engbers JD, Hameed S, Zamponi GW, Turner RW. Regulation of neuronal activity by Cav3-Kv4 channel signaling complexes. Nat Neurosci. 2010a; 13:333–337. [PubMed: 20154682]

Anderson D, Rehak R, Hameed S, Mehaffey WH, Zamponi GW, Turner RW. Regulation of the KV4.2 complex by CaV3.1 calcium channels. Channels (Austin). 2010b; 4:163–167. [PubMed: 20458163]

Barnwell LF, Lugo JN, Lee WL, Willis SE, Gertz SJ, Hrachovy RA, Anderson AE. Kv4.2 knockout mice demonstrate increased susceptibility to convulsant stimulation. Epilepsia. 2009; 50:1741–1751. [PubMed: 19453702]

Bekar LK, Loewen ME, Cao K, Sun X, Leis J, Wang R, Forsyth GW, Walz W. Complex expression and localization of inactivating Kv channels in cultured hippocampal astrocytes. J Neurophysiol. 2005; 93:1699–1709. [PubMed: 15738276]

Bhatt DH, Zhang S, Gan WB. Dendritic spine dynamics. Annu Rev Physiol. 2009; 71:261–282. [PubMed: 19575680]

Birnbaum SG, Varga AW, Yuan LL, Anderson AE, Sweatt JD, Schrader LA. Structure and function of Kv4-family transient potassium channels. Physiol Rev. 2004; 84:803–833. [PubMed: 15269337]

Bourdeau ML, Laplante I, Laurent CE, Lacaille JC. KChIP1 modulation of Kv4.3-mediated A-type K(+) currents and repetitive firing in hippocampal interneurons. Neuroscience. 2011; 176:173–187. [PubMed: 21129448]

NIH-PA Author Manuscript

NIH-PA Author Manuscript

NIH-PA Author Manuscript

Burgoyne RD. Neuronal calcium sensor proteins: generating diversity in neuronal Ca2+ signalling. Nat Rev Neurosci. 2007; 8:182–193. [PubMed: 17311005]

Burgoyne RD, Weiss JL. The neuronal calcium sensor family of Ca2+-binding proteins. Biochem J. 2001; 353:1–12. [PubMed: 11115393]

Carrasquillo Y, Burkhalter A, Nerbonne JM. A-type K+ channels encoded by Kv4.2, Kv4.3 and Kv1.4 differentially regulate intrinsic excitability of cortical pyramidal neurons. J Physiol. 2012; 590:3877–3890. [PubMed: 22615428]

Chavira-Suarez E, Sandoval A, Felix R, Lamas M. Expression and high glucose-mediated regulation of K+ channel interacting protein 3 (KChIP3) and KV4 channels in retinal Muller glial cells. Biochem Biophys Res Commun. 2011; 404:678–683. [PubMed: 21147063]

Chen CP, Lee L, Chang LS. Effects of metal-binding properties of human Kv channel-interacting proteins on their molecular structure and binding with Kv4.2 channel. Protein J. 2006a; 25:345–351. [PubMed: 16951992]

Chen X, Yuan LL, Zhao C, Birnbaum SG, Frick A, Jung WE, Schwarz TL, Sweatt JD, Johnston D. Deletion of Kv4.2 gene eliminates dendritic A-type K+ current and enhances induction of long-term potentiation in hippocampal CA1 pyramidal neurons. J Neurosci. 2006b; 26:12143–12151. [PubMed: 17122039]

Coetzee WA, Amarillo Y, Chiu J, Chow A, Lau D, McCormack T, Moreno H, Nadal MS, Ozaita A, Pountney D, Saganich M, Vega-Saenz dM, Rudy B. Molecular diversity of K+ channels. Ann N Y Acad Sci. 1999; 868:233–285. [PubMed: 10414301]

Conrad KL, Louderback KM, Gessner CP, Winder DG. Stress-induced alterations in anxiety-like behavior and adaptations in plasticity in the bed nucleus of the stria terminalis. Physiol Behav. 2011; 104:248–256. [PubMed: 21396387]

Dabrowska J, Rainnie DG. Expression and distribution of Kv4 potassium channel subunits and potassium channel interacting proteins in subpopulations of interneurons in the basolateral amygdala. Neuroscience. 2010; 171:721–733. [PubMed: 20849929]

Dabrowska J, Hazra R, Ahern TH, Guo JD, McDonald AJ, Mascagni F, Muller JF, Young LJ, Rainnie DG. Neuroanatomical evidence for reciprocal regulation of the corticotrophin-releasing factor and oxytocin systems in the hypothalamus and the bed nucleus of the stria terminalis of the rat: implications for balancing stress and affect. Psychoneuroendocrinology. 2011; 36:1312–1326. [PubMed: 21481539]

De Olmos JS, Heimer L. The concepts of the ventral striatopallidal system and extended amygdala. Ann N Y Acad Sci. 1999; 877:1–32. [PubMed: 10415640]

Decher N, Uyguner O, Scherer CR, Karaman B, Yuksel-Apak M, Busch AE, Steinmeyer K, Wollnik B. hKChIP2 is a functional modifier of hKv4.3 potassium channels: cloning and expression of a short hKChIP2 splice variant. Cardiovasc Res. 2001; 52:255–264. [PubMed: 11684073]

Fontan-Lozano A, Romero-Granados R, del-Pozo-Martin Y, Suarez-Pereira I, gado-Garcia JM, Penninger JM, Carrion AM. Lack of DREAM protein enhances learning and memory and slows brain aging. Curr Biol. 2009a; 19:54–60. [PubMed: 19110430]

Fontan-Lozano A, Romero-Granados R, del-Pozo-Martin Y, Suarez-Pereira I, gado-Garcia JM, Penninger JM, Carrion AM. Lack of DREAM protein enhances learning and memory and slows brain aging. Curr Biol. 2009b; 19:54–60. [PubMed: 19110430]

Gross C, Yao X, Pong DL, Jeromin A, Bassell GJ. Fragile X mental retardation protein regulates protein expression and mRNA translation of the potassium channel Kv4.2. J Neurosci. 2011; 31:5693–5698. [PubMed: 21490210]

Guo JD, Hammack SE, Hazra R, Levita L, Rainnie DG. Bi-directional modulation of bed nucleus of stria terminalis neurons by 5-HT: molecular expression and functional properties of excitatory 5-HT receptor subtypes. Neuroscience. 2009; 164:1776–1793. [PubMed: 19778589]

Guo JD, Hazra R, Dabrowska J, Muly EC, Wess J, Rainnie DG. Presynaptic muscarinic M(2) receptors modulate glutamatergic transmission in the bed nucleus of the stria terminalis. Neuropharmacology. 2012; 62:1671–1683. [PubMed: 22166222]

Hammack SE, Mania I, Rainnie DG. Differential expression of intrinsic membrane currents in defined cell types of the anterolateral bed nucleus of the stria terminalis. J Neurophysiol. 2007; 98:638–656. [PubMed: 17537902]

NIH-PA Author Manuscript

NIH-PA Author Manuscript

NIH-PA Author Manuscript

Hammack SE, Guo J, Hazra R, Dabrowska J, Myers KM, Rainnie DG. The response of neurons in the bed nucleus of the stria terminalis to serotonin: implications for anxiety. Prog Neuropsychopharmacol Biol Psychiatry. 2009; 33:1309–1320. [PubMed: 19467288]

Hazra, R.; Guo, JD.; Rainnie, DG. Differential distribution of neuropeptide mRNA in physiologically defined cell types in the oval subdivision of the anterolateral bed nucleus of stria terminalis. 41st Annual Meeting Society for Neuroscience; Washington, DC. 2011a. UU14

Hazra R, Guo JD, Ryan SJ, Jasnow AM, Dabrowska J, Rainnie DG. A transcriptomic analysis of type I–III neurons in the bed nucleus of the stria terminalis. Mol Cell Neurosci. 2011b; 46:699–709. [PubMed: 21310239]

Holmqvist MH, Cao J, Knoppers MH, Jurman ME, Distefano PS, Rhodes KJ, Xie Y, An WF. Kinetic modulation of Kv4-mediated A-current by arachidonic acid is dependent on potassium channel interacting proteins. J Neurosci. 2001; 21:4154–4161. [PubMed: 11404400]

Jerng HH, Pfaffinger PJ, Covarrubias M. Molecular physiology and modulation of somatodendritic A-type potassium channels. Mol Cell Neurosci. 2004; 27:343–369. [PubMed: 15555915]

Jerng HH, Kunjilwar K, Pfaffinger PJ. Multiprotein assembly of Kv4.2, KChIP3 and DPP10 produces ternary channel complexes with ISA-like properties. J Physiol. 2005; 568:767–788. [PubMed: 16123112]

Jung SC, Kim J, Hoffman DA. Rapid, bidirectional remodeling of synaptic NMDA receptor subunit composition by A-type K+ channel activity in hippocampal CA1 pyramidal neurons. Neuron. 2008; 60:657–671. [PubMed: 19038222]

Kash TL, Nobis WP, Matthews RT, Winder DG. Dopamine enhances fast excitatory synaptic transmission in the extended amygdala by a CRF-R1-dependent process. J Neurosci. 2008; 28:13856–13865. [PubMed: 19091975]

Kim J, Wei DS, Hoffman DA. Kv4 potassium channel subunits control action potential repolarization and frequency-dependent broadening in rat hippocampal CA1 pyramidal neurones. J Physiol. 2005; 569:41–57. [PubMed: 16141270]

Ledo F, Kremer L, Mellstrom B, Naranjo JR. Ca2+-dependent block of CREB-CBP transcription by repressor DREAM. EMBO J. 2002; 21:4583–4592. [PubMed: 12198160]

Lei Z, Deng P, Li J, Xu ZC. Alterations of A-type potassium channels in hippocampal neurons after traumatic brain injury. J Neurotrauma. 2011; 29:235–245. [PubMed: 21895522]

Li C, Dabrowska J, Hazra R, Rainnie DG. Synergistic activation of dopamine D1 and TrkB receptors mediate gain control of synaptic plasticity in the basolateral amygdala. PLoS ONE. 2011; 6:e26065. [PubMed: 22022509]

Lilliehook C, Bozdagi O, Yao J, Gomez-Ramirez M, Zaidi NF, Wasco W, Gandy S, Santucci AC, Haroutunian V, Huntley GW, Buxbaum JD. Altered Abeta formation and long-term potentiation in a calsenilin knock-out. J Neurosci. 2003; 23:9097–9106. [PubMed: 14534243]

Link WA, Ledo F, Torres B, Palczewska M, Madsen TM, Savignac M, Albar JP, Mellstrom B, Naranjo JR. Day-night changes in downstream regulatory element antagonist modulator/potassium channel interacting protein activity contribute to circadian gene expression in pineal gland. J Neurosci. 2004; 24:5346–5355. [PubMed: 15190107]

Lockridge A, Yuan LL. Spatial learning deficits in mice lacking A-type K(+) channel subunits. Hippocampus. 2011; 21:1152–1156. [PubMed: 20857488]

Lockridge A, Su J, Yuan LL. Abnormal 5-HT modulation of stress behaviors in the Kv4.2 knockout mouse. Neuroscience. 2010; 170:1086–1097. [PubMed: 20801198]

Malin SA, Nerbonne JM. Molecular heterogeneity of the voltage-gated fast transient outward K+ current, I(Af), in mammalian neurons. J Neurosci. 2001; 21:8004–8014. [PubMed: 11588173]

Martin EI, Ressler KJ, Jasnow AM, Dabrowska J, Hazra R, Rainnie DG, Nemeroff CB, Owens MJ. A novel transgenic mouse for gene-targeting within cells that express corticotropin-releasing factor. Biol Psychiatry. 2010; 67:1212–1226. [PubMed: 20303068]

McDermott CM, Schrader LA. Activation of kappa opioid receptors increases intrinsic excitability of dentate gyrus granule cells. J Physiol. 2011; 589:3517–3532. [PubMed: 21606111]

Menegola M, Trimmer JS. Unanticipated region- and cell-specific downregulation of individual KChIP auxiliary subunit isotypes in Kv4.2 knock-out mouse brain. J Neurosci. 2006; 26:12137–12142. [PubMed: 17122038]

NIH-PA Author Manuscript

NIH-PA Author Manuscript

NIH-PA Author Manuscript

Muly EC, Maddox M, Smith Y. Distribution of mGluR1alpha and mGluR5 immunolabeling in primate prefrontal cortex. J Comp Neurol. 2003; 467:521–535. [PubMed: 14624486]

Muly EC, Mania I, Guo JD, Rainnie DG. Group II metabotropic glutamate receptors in anxiety circuitry: correspondence of physiological response and subcellular distribution. J Comp Neurol. 2007; 505:682–700. [PubMed: 17948876]

Norris AJ, Foeger NC, Nerbonne JM. Interdependent roles for accessory KChIP2, KChIP3, and KChIP4 subunits in the generation of Kv4-encoded IA channels in cortical pyramidal neurons. J Neurosci. 2010; 30:13644–13655. [PubMed: 20943905]

Rainnie DG. Neurons of the bed nucleus of the stria terminalis (BNST). Electrophysiological properties and their response to serotonin. Ann N Y Acad Sci. 1999; 877:695–699. [PubMed: 10415686]

Rhodes KJ, Carroll KI, Sung MA, Doliveira LC, Monaghan MM, Burke SL, Strassle BW, Buchwalder L, Menegola M, Cao J, An WF, Trimmer JS. KChIPs and Kv4 alpha subunits as integral components of A-type potassium channels in mammalian brain. J Neurosci. 2004; 24:7903–7915. [PubMed: 15356203]

Serodio P, Rudy B. Differential expression of Kv4 K+ channel subunits mediating subthreshold transient K+ (A-type) currents in rat brain. J Neurophysiol. 1998; 79:1081–1091. [PubMed: 9463463]

Serodio P, de Vega-Saenz ME, Rudy B. Cloning of a novel component of A-type K+ channels operating at subthreshold potentials with unique expression in heart and brain. J Neurophysiol. 1996; 75:2174–2179. [PubMed: 8734615]

Sheng M, Tsaur ML, Jan YN, Jan LY. Subcellular segregation of two A-type K+ channel proteins in rat central neurons. Neuron. 1992; 9:271–284. [PubMed: 1497894]

Shibata R, Misonou H, Campomanes CR, Anderson AE, Schrader LA, Doliveira LC, Carroll KI, Sweatt JD, Rhodes KJ, Trimmer JS. A fundamental role for KChIPs in determining the molecular properties and trafficking of Kv4.2 potassium channels. J Biol Chem. 2003; 278:36445–36454. [PubMed: 12829703]

Song WJ. Genes responsible for native depolarization-activated K+ currents in neurons. Neurosci Res. 2002; 42:7–14. [PubMed: 11814604]

Sullivan GM, Apergis J, Bush DE, Johnson LR, Hou M, LeDoux JE. Lesions in the bed nucleus of the stria terminalis disrupt corticosterone and freezing responses elicited by a contextual but not by a specific cue-conditioned fear stimulus. Neuroscience. 2004; 128:7–14. [PubMed: 15450349]

Sun W, Maffie JK, Lin L, Petralia RS, Rudy B, Hoffman DA. DPP6 establishes the A-type K(+) current gradient critical for the regulation of dendritic excitability in CA1 hippocampal neurons. Neuron. 2011; 71:1102–1115. [PubMed: 21943606]

Swanson LW, Petrovich GD. What is the amygdala? Trends Neurosci. 1998; 21:323–331. [PubMed: 9720596]

Walker D, Yang Y, Ratti E, Corsi M, Trist D, Davis M. Differential effects of the CRF-R1 antagonist GSK876008 on fear-potentiated, light- and CRF-enhanced startle suggest preferential involvement in sustained vs phasic threat responses. Neuropsychopharmacology. 2009a; 34:1533–1542. [PubMed: 19078950]

Walker DL, Miles LA, Davis M. Selective participation of the bed nucleus of the stria terminalis and CRF in sustained anxiety-like versus phasic fear-like responses. Prog Neuropsychopharmacol Biol Psychiatry. 2009b; 13:1291–1308. [PubMed: 19595731]

Weitlauf C, Egli RE, Grueter BA, Winder DG. High-frequency stimulation induces ethanol-sensitive long-term potentiation at glutamatergic synapses in the dorsolateral bed nucleus of the stria terminalis. J Neurosci. 2004; 24:5741–5747. [PubMed: 15215296]

Wu LJ, Mellstrom B, Wang H, Ren M, Domingo S, Kim SS, Li XY, Chen T, Naranjo JR, Zhuo M. DREAM (downstream regulatory element antagonist modulator) contributes to synaptic depression and contextual fear memory. Mol Brain. 2010; 3:3. [PubMed: 20205763]

Xiong H, Kovacs I, Zhang Z. Differential distribution of KChIPs mRNAs in adult mouse brain. Brain Res Mol Brain Res. 2004; 128:103–111. [PubMed: 15363885]

Yu FH, Yarov-Yarovoy V, Gutman GA, Catterall WA. Overview of molecular relationships in the voltage-gated ion channel superfamily. Pharmacol Rev. 2005; 57:387–395. [PubMed: 16382097]

NIH-PA Author Manuscript

NIH-PA Author Manuscript

NIH-PA Author Manuscript

Zagha E, Ozaita A, Chang SY, Nadal MS, Lin U, Saganich MJ, McCormack T, Akinsanya KO, Qi SY, Rudy B. DPP10 modulates Kv4-mediated A-type potassium channels. J Biol Chem. 2005; 280:18853–18861. [PubMed: 15671030]

Zhang Y, Su P, Liang P, Liu T, Liu X, Liu XY, Zhang B, Han T, Zhu YB, Yin DM, Li J, Zhou Z, Wang KW, Wang Y. The DREAM protein negatively regulates the NMDA receptor through interaction with the NR1 subunit. J Neurosci. 2010; 30:7575–7586. [PubMed: 20519532]

Zhao C, Wang L, Netoff T, Yuan LL. Dendritic mechanisms controlling the threshold and timing requirement of synaptic plasticity. Hippocampus. 2011; 21:288–297. [PubMed: 20087888]

Zimmerman JM, Maren S. The bed nucleus of the stria terminalis is required for the expression of contextual but not auditory freezing in rats with basolateral amygdala lesions. Neurobiol Learn Mem. 2011; 95:199–205. [PubMed: 21073972]

NIH-PA Author Manuscript
NIH-PA Author Manuscript
NIH-PA Author Manuscript

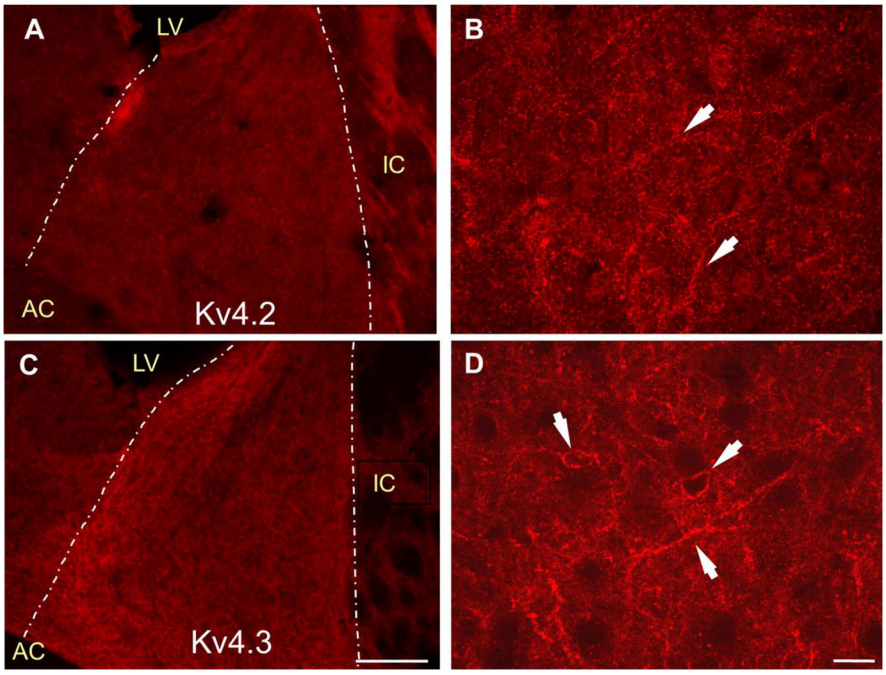

Figure 1.

Photomicrographs showing immunoreactivity for the Kv4 α-subunits of the A-type potassium channel in the BNST. **A:** At low magnification (10×), the Kv4.2 α-subunit was seen to be highly expressed in the $BNST_{ALG}$ (outlined by dashed lines). **B:** At higher magnification (63×), Kv4.2 was seen to be expressed mainly as punctate labeling in the neuropil throughout the $BNST_{ALG}$. **C:** At low magnification (10×) the Kv4.3 α-subunit also showed high immunoreactivity in the $BNST_{ALG}$ (outlined). **D:** At higher magnification (63×) Kv4.3 was seen to be highly expressed in processes and cell membranes of BNST neurons (arrows) as well as in the neuropil. AC, anterior commissure; LV, lateral ventricle; IC, internal capsule. Scale bars =100 μm in C; 10 μm in D. [Color figure can be viewed in the online issue, which is available at wileyonlinelibrary.com.]

NIH-PA Author Manuscript
NIH-PA Author Manuscript
NIH-PA Author Manuscript

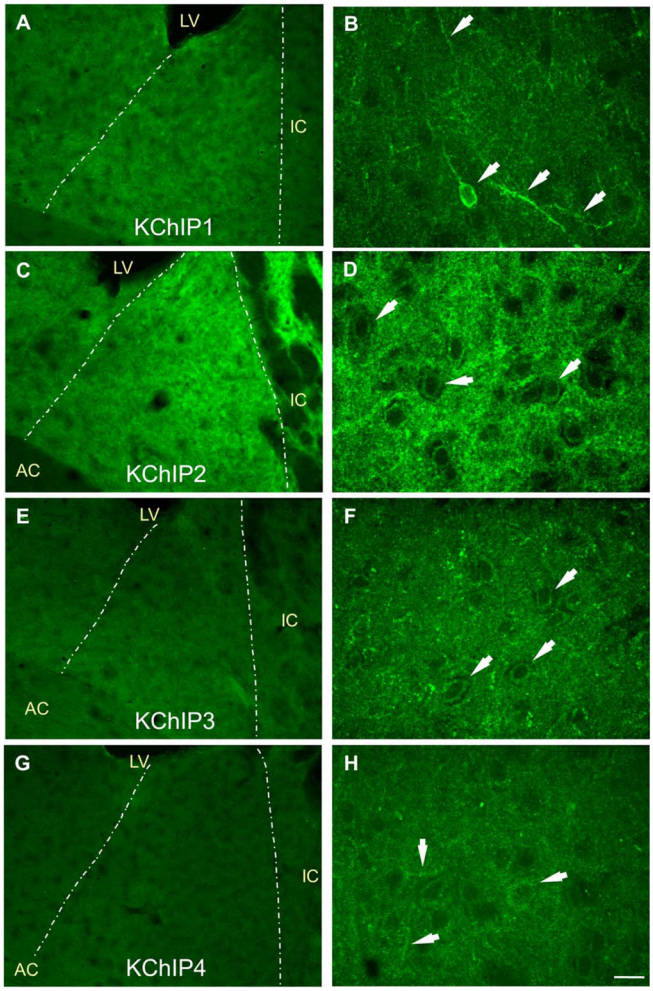

Figure 2.

Photomicrographs showing immunoreactivity for the β-subunits of the Kv4 potassium channels, KChIP1-KChIP4 in the $BNST_{ALG}$. **A–G**: At low magnification (10×), all four KChIPs were seen to be expressed in the BNST with the highest immunoreactivity observed for KChIP2 (C), moderate expression for KChIP1 (A) and KChIP3 (E), and the lowest expression for KChIP4 (G). A,B: Moderate immunoreactivity was observed for KChIP1 in the BNST with the highest expression seen in the soma and processes of isolated BNST neurons (arrows), as well as punctate label in the neuropil. C,D: KChIP2 showed the highest immunoreactivity in the BNST. KChIP2 immunolabeling was seen in the neuropil where it appeared as a strong punctate immunoreactivity. Furthermore, rings of lighter immunoreactivity were observed that appeared to encircle the nuclei of BNST neurons (arrows). E,F: KChIP3 showed moderate punctate neuropil immunoreactivity in the BNST, as well as apparent perinuclear rings in BNST cell bodies (arrows). G,H: KChIP4 showed the weakest immunoreactivity in the BNST. Diffuse punctate immunolabeling was observed throughout the neuropil, as well as in some processes and cell bodies (arrows). Left panels 10×, right panels 63×. Scale bar =100 μm; for left panels; 10 μm for right panels. [Color figure can be viewed in the online issue, which is available at wileyonlinelibrary.com.]

NIH-PA Author Manuscript
NIH-PA Author Manuscript
NIH-PA Author Manuscript

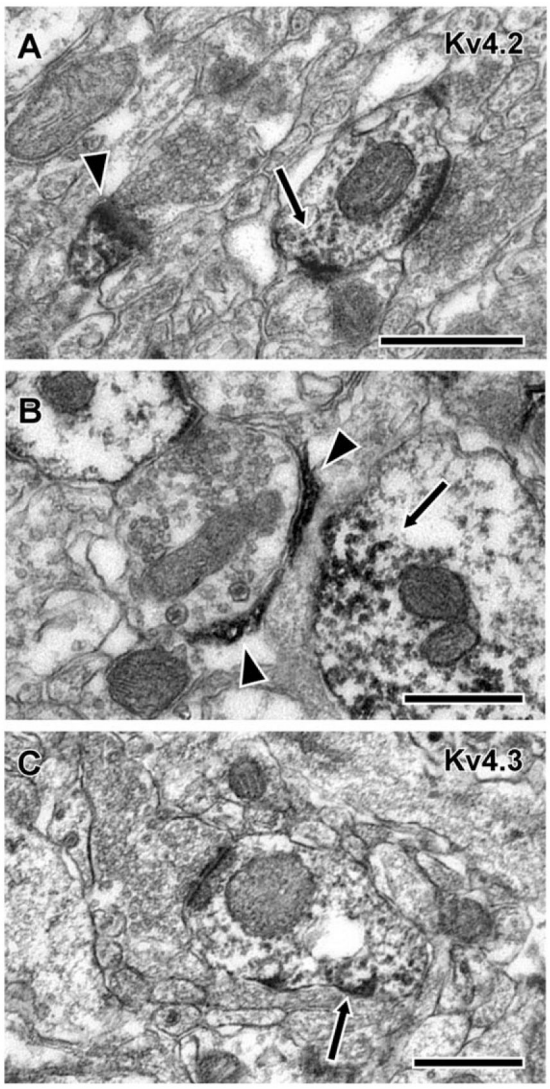

Figure 3.

Subcellular distribution of Kv4.2 and Kv4.3 α subunits in the $BNST_{ALG}$. **A:** Kv4.2 labeling was observed primarily in dendrites (arrow) with spines (arrowhead) labeled as well. **B:** Kv4.2 label was also seen in glial profiles, often wrapping around axon terminals (arrowheads). A labeled dendritic profile is also indicated with an arrow. **C:** Arrow shows a Kv4.3-labeled dendrites in the BNST. Scale bars =500 nm.

NIH-PA Author Manuscript
NIH-PA Author Manuscript
NIH-PA Author Manuscript

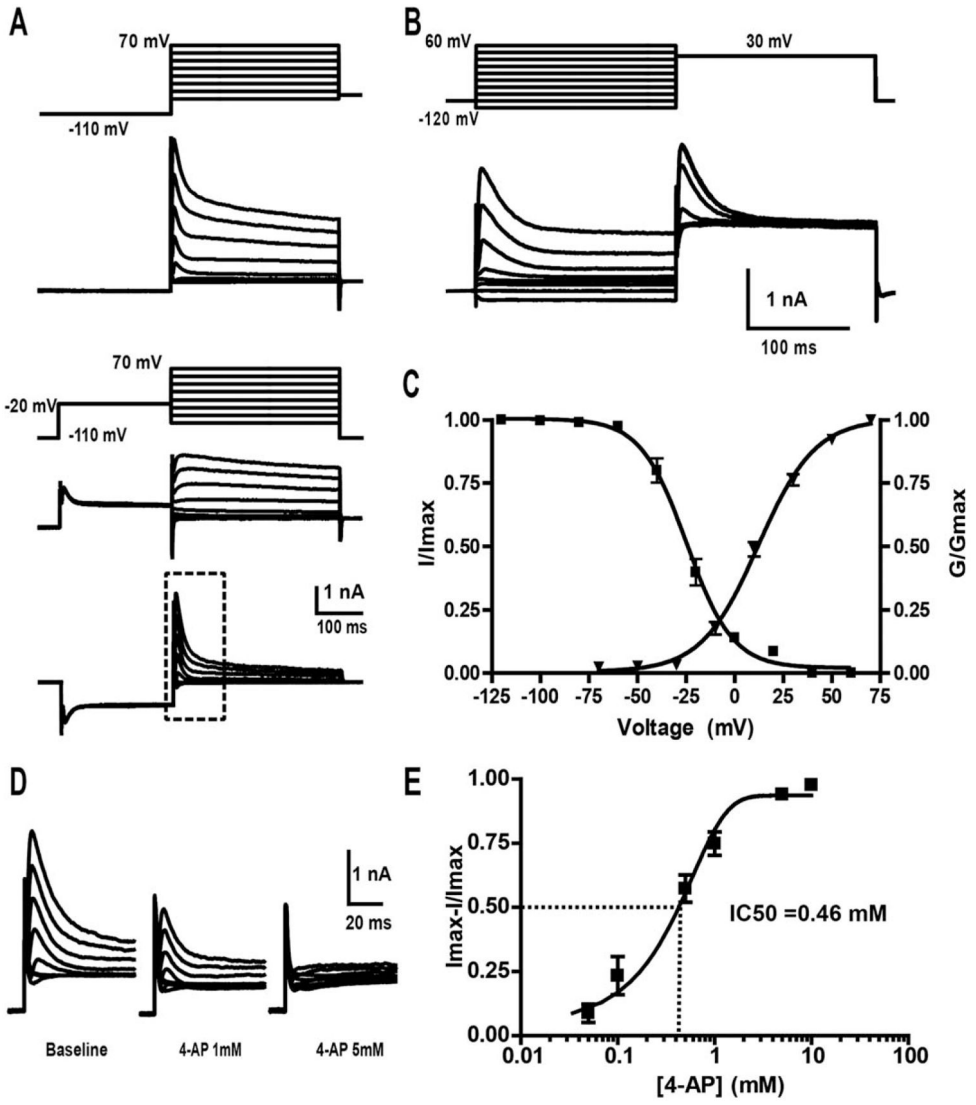

Figure 4.

Blockade of I_A in $BNST_{ALG}$ neurons requires low mM extracellular concentrations of the channel blocker 4-aminopyridine (4-AP). **A:** Representative traces showing the voltage clamp traces used for digital subtraction and isolation of I_A activation properties. Isolated I_A is illustrated in the bottom trace. **B:** Representative traces showing the voltage clamp traces used for isolation of I_A inactivation properties. **C:** Group data showing the voltage dependence of I_A activation and inactivation. **D:** Application of the nonspecific I_A channel blocker 4-AP dose-dependently decreased I_A amplitude, with complete blockade observed with 5 mM 4-AP. **E:** A dose–response curve for the 4-AP effect revealed an IC_{50} of 460 μM.

NIH-PA Author Manuscript

NIH-PA Author Manuscript

NIH-PA Author Manuscript

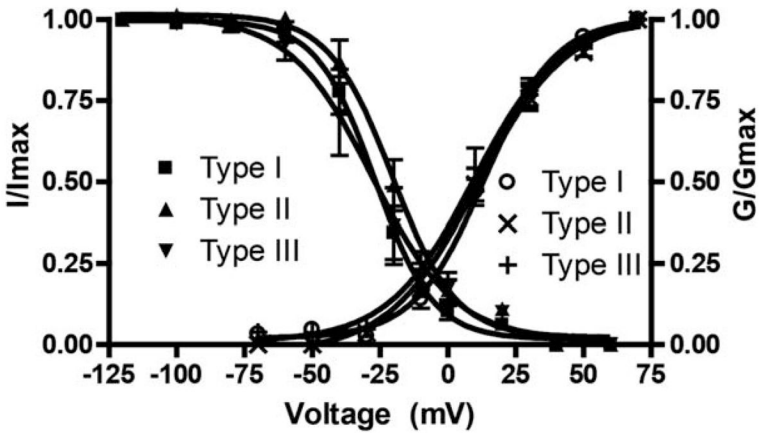

Figure 5.

Plots of steady-state voltage-dependent activation and inactivation of I_A in Type I–III $BNST_{ALG}$ neurons. Isolated I_A was obtained from three physiologically defined $BNST_{ALG}$ neurons. Normalized peak I_A currents (activation) or conductance (inactivation) were plotted as a function of command potential. Steady-state activation curves (open circle, cross, plus, for Type I–III neurons, respectively), and inactivation curves (filled square, upward and downward triangles for Type I–III neurons, respectively) were fit with Boltzmann equation. No significant difference was found among the three cell types for half maximal activation or inactivation. (*n* =13, 10, and 7 for Type I–III neurons, respectively).

NIH-PA Author Manuscript

NIH-PA Author Manuscript

NIH-PA Author Manuscript

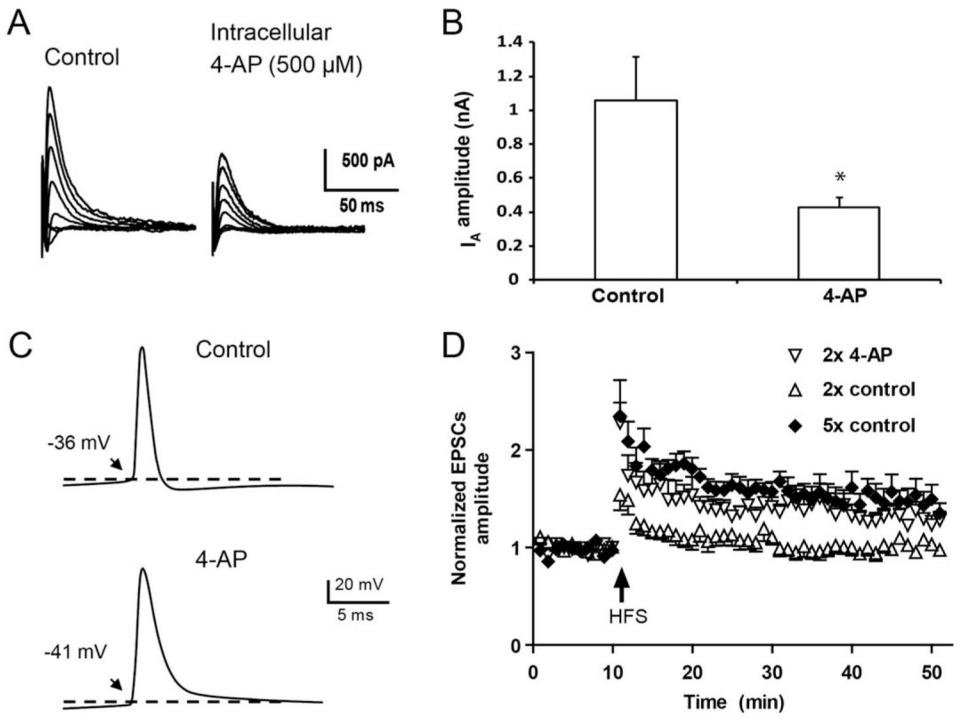

Figure 6.

Reducing I_A in $BNST_{ALG}$ neurons with intracellular 4-AP lowers the threshold for LTP induction. **A:** Representative traces showing that intracellular application of 4-AP (500 μM) decreased the amplitude of the digitally isolated I_A. **B:** Bar graph summarizing the group data for the effects of intracellular 4-AP on I_A amplitude (*$P < 0.05$ compared to baseline). **C:** Intracellular 4-AP changed the action potential properties, decreasing the threshold, increasing the decay time and half width, and eliminating the afterhyperpolarization. **D:** 5× HFS, but not 2× HFS could induce LTP in control $BNST_{ALG}$ neurons. However, in neurons recorded with intracellular 4-AP (500 μM), 2× HFS successfully induced LTP.

NIH-PA Author Manuscript

NIH-PA Author Manuscript

NIH-PA Author Manuscript

TABLE 1

PCR Primers Used

Genes	Accession #	PCR product size (bp)
Kv1.4	X16002	434
Kv3.4	X62841	676
Kv4.1	M64226	467
Kv4.2	S64320	265
Kv4.3	U42975	296/386
KChIP1	AY082657	239
KChIP2	AF269283	324/270/174
KChIP3	NM_032462	197
KChIP4	AF345444	377/275

NIH-PA Author Manuscript

NIH-PA Author Manuscript

NIH-PA Author Manuscript

TABLE 2

Antibodies Used in Immunohistochemistry and Western Blots

Antibody	Antigen	Company	Catalog number	Host
Kv4.2 1.03 mg/ml	synthetic peptide from amino acids 209–225 (extracellular S1–S2 loop) of rat Kv4.2	UC Davis/NIH NeuroMab Facility (Davis, CA) Antibodies Incorporated	75-016 Clone K57/1	Mouse monoclonal
Kv4.3 1.04 mg/ml	fusion protein of amino acids 415–636 of rat Kv4.3 (C-terminal)	UC Davis/NIH NeuroMab Facility (Davis, CA) Antibodies Incorporated	75-017 Clone K75/41	Mouse monoclonal
KChIP1 1.05 mg/ml	full-length fusion protein of amino acids 1–216 of rat KChIP1b	UC Davis/NIH NeuroMab Facility (Davis, CA) Antibodies Incorporated	75-003 Clone K55/7	Mouse monoclonal
KChIP2 1.00 mg/ml	full-length fusion protein of amino acids 1–252 of rat KChIP2b	UC Davis/NIH NeuroMab Facility (Davis, CA) Antibodies Incorporated	75-004 Clone K60/73	Mouse monoclonal
KChIP3 1.02 mg/ml	full-length fusion protein of amino acids 1–256 of rat KChIP3	UC Davis/NIH NeuroMab Facility (Davis, CA) Antibodies Incorporated	75-005 Clone 66/38	Mouse monoclonal
KChIP4 1.00 mg/ml	full-length protein from amino acids 1–251 of human KChIP4	Abcam (Cambridge, MA)	ab57830	Mouse monoclonal

NIH-PA Author Manuscript
NIH-PA Author Manuscript
NIH-PA Author Manuscript

TABLE 3

Cell Type-Selective Expression of Kv4 and KChIP mRNA Transcripts in the $BNST_{ALG}$

Cell type	Kv4.1	Kv4.2	Kv4.3	KChIP1	KChIP2	KChIP3	KChIP4	N
I	0	9	9	0	0	9	6	9
II A	0	14	0	0	0	14	0	14
II B	0	12	0	0	0	0	12	12
II C	0	0	14	14	14	14	14	14
III	0	12	0	0	12	4	12	12

The table shows the number of neurons of each $BNST_{ALG}$ Type I–III subtype expressing mRNA transcripts for the Kv4 family of I_A α subunits and their associated KChIPs. Far right column shows the total number of neurons sampled for each subtype.

NIH-PA Author Manuscript NIH-PA Author Manuscript NIH-PA Author Manuscript

TABLE 4

Functional Properties of I_A in Type I–III Neurons of the $BNST_{ALG}$

		Total	Type I	Type II	Type III
Activation	$V_{1/2}$ (mV)	12.2±1.1	13.6±1.4	11.0±2.1	9.4±2.5
	k	14.6	12.9	16.4	15.7
Inactivation	$V_{1/2}$ (mV)	−24.8±1.2	−26.9±1.6	−20.6±1.7	−27.7±3.3
	k	−11.8	−10.7	−11.7	−15.3
I_A amplitude (pA)		592±82	503±130	754±159	526±105
Tau of decay (ms)		25.8±0.9	27.3±3.1	24.7±3.0	26.0±1.7
n		30	13	10	7

$V_{1/2}$ = the voltage of half-maximal activation or inactivation; *k* =slope; Tau =time constant for the decay phase of I_A.I_A amplitude and Tau were determined at command steps to 30 mV.

J Comp Neurol. Author manuscript; available in PMC 2014 September 04.

NIH-PA Author Manuscript NIH-PA Author Manuscript NIH-PA Author Manuscript

TABLE 5

Effects of Intracellular 4-AP on Membrane Properties of BNST Neurons

				Spike					
Cell type	**Treatment**	**RMP (mV)**	**Rin (MΩ)**	**Amplitude (mV)**	**Half Width (ms)**	**Rise Time (ms)**	**Decay Time(ms)**	**Threshold (mV)**	**fAHP (mV)**
Type I/II	Control	−58.3±1.1	400±55	73.4±2.6	0.95±0.06	0.38±0.02	1.0±0.1	−36.6±0.6	−7.2±1.7
	4-AP	−56.1±1.3	421±72	80.1±2.4	1.34±0.04**	0.47±0.01**	1.9±0.2**	−41.1±0.8**	−1.2±1.0**
Type III	Control	−63.9±1.4	254±60	71.2±2.9	1.12±0.04	0.45±0.03	1.1±0.1	−33.2±1.0	−3.4±0.5
	4-AP	−63.3±1.8	349±111	83.8±3.9*	1.56±0.09**	0.48±0.03	2.4±0.3**	−36.8±1.1*	−1.5±2.7

$BNST_{ALG}$ neurons were recorded with control patch solution or patch solution containing 4-AP (500 μM).

*, ** $P < 0.05$ and 0.01, respectively, compared to control group. RMP =resting membrane potential. Rin =membrane input resistance. fAHP =fast afterhyperpolarization.